Journal of Physics: Theories and Applications E-ISSN: 2549-7324 / P-ISSN: 2549-7316
J. Phys.: Theor. Appl. Vol. 4 No. 1 (2020) 36-47 doi: 10.20961/jphystheor-appl.v4i1.40350

Study of co-precipitated nanomaterials magnetic $Mn_xCo_{1-x}Fe_2O_4$ (with x = 0.50 & 0.75) for Photocatalyst Application in MB degradation

Wahid Sidik Sarifuddin[a], Utari and Budi Purnama[b]

Departemen of Physics, Post Graduate Program, Sebelas Maret University, Jl. Ir. Sutami 36A Kentingan, Jebres, Surakarta 57126, Indonesia

E-mail: [a]wahid.elsyarif@gmail.com, [b]bpurnama@gmail.com

Received 27 February 2020, Revised 5 January 2021, Published 29 March 2020

Abstract: The crystalline structure and magnetic properties of $Mn_{1-x}Co_xFe_2O_4$ (x = 0 & 0.25) was studied in this report. The ferrite materials were synthesized by the chemical co-precipitation method and calcinated at 1000°C for 5 hours. The obtained materials were characterized by FTIR, XRD and VSM, and for photocatalytic activity was measured by UV-Vis spectrometer. Vibration bands at tetrahedral and octahedral site were corresponded by ϑ_1 = 581.56 cm^{-1} and ϑ_2 = 465.83 cm^{-1} and 474.51 cm^{-1} . The obtained ferrite were confirmed by XRD as spinel structure and shown that the addition of number of Mn decreased crystallite size *(D)* and x-ray density (ρ_x), but lattice constants *(a)* increased. The crystallite size of samples with x = 0.50 was 34.85 nm, and x = 0.75 was 32.17 nm. The magnetic properties of nanoparticles shown that magnetization saturation *(Ms)* from 42.05 emu/g to 54.16 emu/g increased with the addition of number of Mn. The coercive field (H_c) decreased from 408.27 Oe to 258.37 Oe. Photocatalytic activity was observed by UV-Vis spectrometer, where percentage of MB degradation *(E)* increase with the addition of number on Mn from 49.08% to 69.06%, either rate constant *(k_{app})* and half life time *($t_{1/2}$)*. Furthermore, ferrite material base Mn-Co-ferrite has good characteristic to applied for photocatalyst.

Keyword : crystalline structure, magnetic properties, manganese cobalt ferrite, chemical co-precipitation, photocatalyst, Methylene Blue

1. Introduction

The ferrite materials have been studied because their magnetic properties and nano-sized crystallite known as magnetic nanomaterials (Enrico, 2017; Atif et al., 2016). The crystal structure of this material is a cubic spinel with a general formation MFe2O4, with "M" is a divalent cation such as Cu2+, Zn2+, Co2+, Mn2+, Ni2+, Mg2+, and others, and a trivalent Fe3+ metal ion. There is some spinel variation, normal spinel ferrite have M2+ in tetrahedral site and Fe3+ in octahedral site. Spinel ferrites with other formation trivalent ions (Fe3+) are equally divided between tetrahedral and octahedral site, and divalent ions (M2+) are on octahedral site known as inverse spinel (Kotnala & Shah).

Some physical characteristics from this ferrite material can be modified by substituting another metals (Boda et al., 2019; Swatsitang et al 2016).

The new magnetic and others physical properties obtained from spinel ferrites which is the combination of Mn and Co in attract the attention of many researchers (Nasrin et al, 2019; Becyte et al., 2015; Jabbar et al., 2019). The purpose is to expand the application of this material, so it can be more appropriate in the utilization of human life. Manganese ferrite has low coercivity and high saturation magnetization (Kotnala & Shah), and cobalt ferrite has high magneto-crystalline anisotropy, high coercivity (Liu et al., 2006), high curie temperatures, moderate saturation magnetization, good mechanical and chemical properties (Purnama et al., 2018; Vlazan et al., 2014).

The spinel ferrite materials has been widely implemented in the human life, i.e. for the industry (Caltun et al., 2007), drug delivery (Marcu et al., 2013), medical treatment (Doaga et al., 2013), antibacteria (Ashour et al., 2018), photocatalyst (Magone et al., 2018).

Photocatalysis is one of wastewater treatment. This technique is known as the advanced oxidation process, which toxic organics in water are destroyed without transferring into other form (Mota et al., 2009).

The water pollution have been great issue in the whole world. This problem requires serious attention and treatment because water is primary need for human and animal life (Montgomery & Elimelech, 2007). There are many material that can contaminate water around people, such as heavy metal, plastic, anorganic-organic pollutants, dyes, etc (Forgacs et al., 2004; Sonu, 2019).

Methylene blue (MB) Dyes are common matter that applied in the industries which used colouring process for their product (Sonu, 2019). The impact from this activity is waste water and aquatic pollution. The chemical material were contained in dyes solution can be toxic for human and animal (Masunga et al., 2019). Therefore, photocatalysis can be applied for treatment the wastewater, and this technique use the adsorbents for remove dyes. Thus, ferrite material can use for this photocatalys process.

There are some methods that can be used in the synthesis of spinel ferrites material such as mechano-chemical synthesis (Becyte et al., 2015), combustion method, hydrothermal method, mechanical alloying (Vlazan et al., 2014; Hou et al., 2010; Koseoglu et al., 2012; Mostafa et al., 2013), sol-gel method (Xi & Xi, 2016), solid-state (Tsay et al., 2014), chemical co-precipitation (Nasrin et al., 2019; Lungu et al., 2015; Karaagac et al., 2019). This paper reported obtaining of manganese cobalt ferrite ($Mn_xCo_{1-x}Fe_2O_4$) with $x = 0.50$ & 0.75 synthesized by chemical co-precipitation method.

The obtained materials are investigated by FTIR, X-ray diffraction (XRD), magnetic measurements (VSM), and UV-Vis spectrometer. This paper explained the study about effect of addition of Mn^{2+} cations in the substitution of manganese cobalt ferrite system. The substitution cations between Mn and Co causes the structure of crystal, magnetic properties in the ferrite system, and photocatalytic activity in MB degradation.

2. Experimental work

2.1. Synthesis of nanomagnetic materials

The method for synthesized nanomagnetic materials (MnxCo1-xFe2O4) was chemical co-precipitation. The main ingredients used were Mn (NO3)2·4H2O (EMSURE 99%, Merck Germany), Co(NO3)2·6H2O (EMSURE 99%, Merck Germany), Fe(NO3)3·9H2O (EMSURE 99%, Merck Germany), and the titration using 4.8 M NaOH from 6 M NaOH (EMSURE 99%, Merck Germany). The calculation of stochiometric were Mn : Co : Fe = x : 1-x : 2, with x = 0.50 and 0.75.

The first step was the main ingredients (Mn, Fe, Co) are dissolved in 200 ml of Aquades and stirred in 300 rpm for 15 minutes. Then, the solution was heated to 95oC and titrated drop by drop with 100 ml NaOH solution. The obtained solution from the titration process is deposited for 12 hours. The precipitate formed is washed 3 times with Ethanol and dried at 100oC for 12 hours. The obtained solids are manually pulverized for 45 minutes and calcinated for 5 hours at 1000oC. Finally, the sample is manually pulverized again for 60 minutes.

2.2. Characterization and calculation

The obtained samples were characterized using FTIR, X-Ray Diffractometer (XRD), Vibrating Sample Magnetometer (VSM), and UV-Vis spectrometer.

FTIR measurements used to identifying Metal oxide bond in the samples and the effect from addition Mn content in the subitution of ferrite system with calculation of force constants. The force constant for the tetrahedral (F_t) and octahedral site (F_o) calculate by formula

$$F_t = 4\pi^2 c^2 \mu \vartheta_1^2 \quad (1)$$

$$F_o = 4\pi^2 c^2 \mu \vartheta_2^2 \quad (2)$$

c is the velocity of light = 2.99 x 10^{10} cm/s, μ is the reduced mass of Fe^{3+} and O^{2-} ions = 2.60 x 10^{-23} g. ϑ_1 and ϑ_2 are FTIR absorption bands which correlated with stretching of the bonds Metal – oxygen in the tetrahedral and octahedral sites.

XRD calculation, crystallite size *(D)* and lattice constant *(a)* were determined using the Scherrer's formula for the highest peak [3 1 1] with λ of the CuKα wavelength is 1.54251 Å.

Nasrin *et al.* [6] reported tha tetrahedral (r_A)and octahedral (r_B) ionic radii determined by Standley's equation. X-ray density was determined by the formula:

$$\rho_x = \frac{8M}{Na^3} \quad (3)$$

M is the relative molecular mass of the sample, *N* is the Avogadro number, and *a* is the lattice constant.

Finally, the magnetic properties of manganese cobalt ferrites ($Mn_xCo_{1-x}Fe_2O_4$) were determined using hysteresis curves of Magnetization field (*M-H*).

2.3. Photocatalytic measurement

Photocatalytic activity studies were carried out at the room temperature. the sample of 10 mg manganese cobalt ferrite was placed in 15 ml of an aqueous solution of MB (10 ppm). The wavelength of MB, λ = 664 nm. The sample was irradiated using UV lamp and stirring in magnetic stirred for 300 seconds, this step was carried out in dark box. The obtained aqueous solution measured by UV-Vis, the results were compared with pure MB.

Photocatalytic efficiency (E) of MB dyes solution removal calculated by:

$$E = \left(1 - \frac{C_t}{C_0}\right) \times 100\% \quad (4)$$

C_0 is the initial concentration of MB before reaction and C_t is the concentration of MB at certain time after reaction. The photocatalytic kinetic of dye solution can be calculated by the Langmuir-Hinshel Wood model,

$$\ln \frac{C_0}{C_t} = k_{app} \cdot t \quad (5)$$

k_{app} is the apparent rate constant, t is time of reaction. The pseudo-first-order reaction half life time ($t_{1/2}$) was calculated with formula

$$t_{1/2} = \frac{\ln 2}{k_{app}} \quad (6)$$

3. Results & Discussions

In $CoFe_2O_4$ which has an structure inverse cubic spinel, the divalent ions Co^{2+} & Mn^{2+}occupy on site B (octahedral), and trivalent Fe^{3+} ions occupy on the A (tetrahedral) & B site (Kotnala & Shah). The $MnFe_2O_4$ which has a partially inverse cubic spinel, the trivalent Fe^{3+} ions occupy the A & B site, and divalent Mn^{2+} ions occupy the site B and the most cations are in A site (Atif et al., 2016).

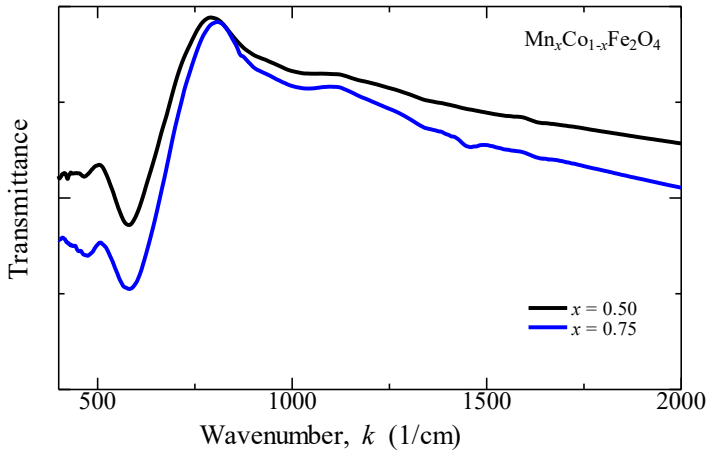

Figure 1 the FTIR spectra of the $Mn_xCo_{1-x}Fe_2O_4$ with x = 0.50 and 0.75.

Figure 1 shows the FTIR spectra for cations in ferrite crystal of $Mn_xCo_{1-x}Fe_2O_4$. The vibrations of metal ions for ferrite crystal lattice usually in range 200-800 cm-1 (Gul & Akhtar, 2018; Arshad et al., 2019). The bands occurred at range 400-470 cm^{-1} revealed the octahedral band of Co/Mn-O (Samavati & Ismail, 2017; Ghahfarokhi & Shobegar,

2017) and another bands occurred at range 500-600 cm^{-1} revealed the tetrahedral band of Fe-O (Saputro et al., 2019).

Table 1. The absorption band and force constant at tetrahedral & octahedral sites of $Mn_xCo_{1-x}Fe_2O_4$

x	ϑ_1 (cm^{-1})	ϑ_2 (cm^{-1})	F_t (dyne/cm)	F_o (dyne/cm)
0.50	581.56	465.83	3.10 x 10^5	1.99 x 10^5
0.75	581.56	474.51	3.10 x 10^5	2.06 x 10^5

The absorption for the manganese cobalt ferrite with x = 0.50 and x = 0.75 were at ϑ_1 = 581.56 cm^{-1} as seen in the Table 1. From the result of the sample is known that addition Mn content in manganese cobalt ferrite sample has no change on the shift of wave numbers on tetrahedral site as shown at force constant (F_t) = 3.10 x 10^5 dyne/cm for all samples.

In octahedral site, ϑ_2 = 465.83 cm^{-1} and 474.51 cm^{-1} for x = 0.50 and 0.75. The force constant (F_o) = 1.99 x 10^5 dyne/cm increase to 2.06 x 10^5 dyne/cm with the addition of Mn contents, the total force constant enhancement of 0.08 dyne/cm attribute the redistribution and substitution of divalent cations (Mn^{2+} and Co^{2+}), which indicate that the treatment of number of Mn ions affect physical properties at octahedral site (Saputro et al., 2019).

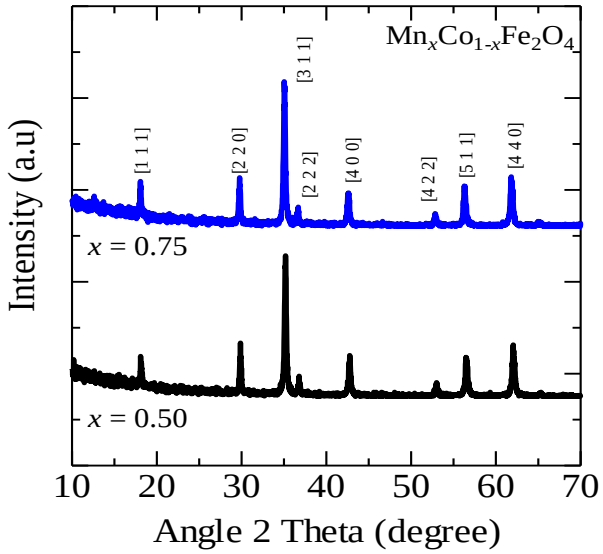

Figure 2. the XRD pattern of the $Mn_xCo_{1-x}Fe_2O_4$ with x = 0.50 and 0.75.

Figure 2 shows the XRD pattern of the sample $Mn_xCo_{1-x}Fe_2O_4$, and the pattern corresponds to the ICDD 22-1086 for Cobalt Ferrite ($CoFe_2O_4$) and ICDD 74-2403 for $MnFe_2O_4$ crystal structure with x = 0.50 and 0.75 and confirmed the formation cubic spinal structure *Fd3m* space group. In the sample x = 0.50 has a peak (3 1 1) which is higher than sample x = 0.75.

Table 2 shows the results of the analysis based on Figure 2 by calculation from the Scherrer's formula. Table 2 shows the lattice constant *(a)* and lattice strain (ε) increase in

the addition of Co content, while X-ray density *(ρ_x)* and crystallite size *(D)* decrease. Co^{2+}, Mn^{2+}, and Fe^{3+} ions can occupy site A (tetrahedral) or site B (octahedral) or both which affect the lattice constant *(a)* (Atif et al., 2016).

Table 2. The results of crystalline parameter of $Mn_xCo_{1-x}Fe_2O_4$

	Magnitude of x	
	***x* = 0.50**	***x* = 0.75**
Lattice constant, ***a*** (x 10^{-10} m)	8.46	8.50
Crystallite size, ***D*** (nm)	34.85	32.17
X-Ray density, $\boldsymbol{\rho_x}$ (g/cc)	5.10	5.01
Ionic Radii Octahedral, $\boldsymbol{r_B}$ (x 10^{-11} m)	7.66	7.75

Addition of Mn^{2+} content on the previous manganese cobalt ferrite causes Co^{2+} ions in B site substituted by Mn^{2+} increase, and the size of Co^{2+} is smaller than Mn^{2+} (Gul & Akhtar, 2018). Thus, The sublattice on-site B will increase, it can be shown by increasing ionic radii octahedral from 7.66 x 10^{-11} m to 7.75 x 10^{-11} m. Sublattice changes at the site B (octahedral) caused increase from 8.46 x 10^{-10} m to 8.50 x 10^{-10} m in lattice constant.

The substitution of Mn^{2+} ions into the manganese cobalt ferrite system are also affect the decrease in the density value of $Mn_xCo_{1-x}Fe_2O_4$ *(ρ_x)* from 5.096 g/cc to 5.007 g/cc, where the density of Co^{2+} and Fe^{3+} are greater than Mn^{2+} (Flores, 2015), so that addition of Mn^{2+} contents will cause the density of $Mn_xCo_{1-x}Fe_2O_4$ with x = 0.50 greater than x = 0.75.

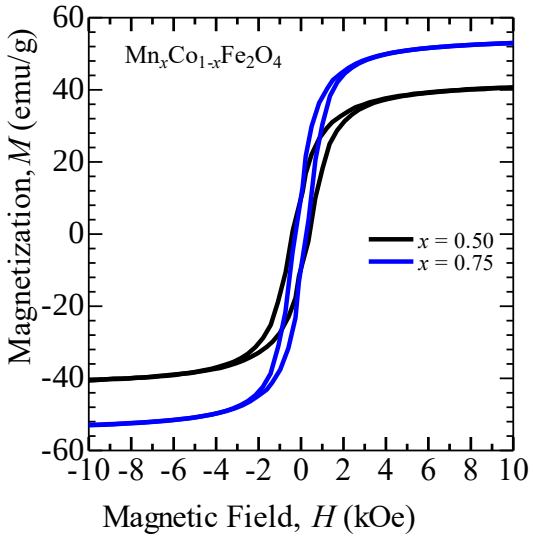

Figure 3. *M-H* curve of the co-precipitated $Mn_xCo_{1-x}Fe_2O_4$ with x = 0.50 and 0.75.

Figure 3 shows the *M-H* curve from the sample $Mn_xCo_{1-x}Fe_2O_4$ with x = 0.50 and 0.75, the curve with x = 0.50 is more linear than the sample with x = 0.75. The Magnetization saturation and magnetization remanent in the sample $Mn_xCo_{1-x}Fe_2O_4$ increase with the rise of presence of manganese, but neither with coercive field.

Table 3. Magnetic properties of $Mn_xCo_{1-x}Fe_2O_4$

	Magnitude of *x*	
	***x* = 0.50**	***x* = 0.75**
Magnetization Saturation, *Ms*(emu/g)	42.05	54.16
Coercive field, *Hc* (Oe)	408.27	258.37
Magnetization Remanent, *Mr* (emu/g)	9.84	9.93

Table 3 shows saturation magnetization increased from 42.05 emu/g to 54.16 emu/g. The net magnetic material depends on distribution and substitution cation among tetrahedral and octahedral sublattice (Ahalya et al., 2014; Cojocariu et al., 2012). The net magnetic moment for Co^{2+}, Mn^{2+}, and Fe^{3+} are 3 μ_B, 5μ_B, and 5 μ_B [23]. This also caused by increasing magnetic moments with the addition of presence of Mn^{2+} ions in B site. According to the theory of molecular field, the total net magnetization at temperature *T*, i.e. $M(T) = M_B(T) - M_A(T)$, where $M_B(T)$ is the magnetization in B site (octahedral) and $M_A(T)$ is the magnetization in A site (tetrahedral).

Thus, the magnetic interaction contributes to the value of magnetic properties. The magnetic moments can be caused interaction of metal ions on tetrahedral and octahedral site [3]. The addition of number of Mn^{2+} ions to the manganese cobalt ferrite system caused interaction between Fe^{3+} ions at the same site tetrahedral and octahedral resulted A-A and B-B interactions and substitution of Mn^{2+} ions to Co^{2+} ions in octahedral site resulted B-B interactions (Nasrin et al., 2019).

As the addition of manganese presence, the coercivity decreased from 408.27 Oe to 258.37 Oe. This suggests that the samples tend to show superparamagnetic behavior.

Generally, photocatalytic process have three steps : (i) the photon absorption with higher energy compared to band gap of nanoparticle, (ii) the separation of photogenerated pairs of electron (e^-) and hole (h^+), recombination, migration, or generation, (iii) the redox reaction on the nanoparticle surface (Pakzad et al., 2019).

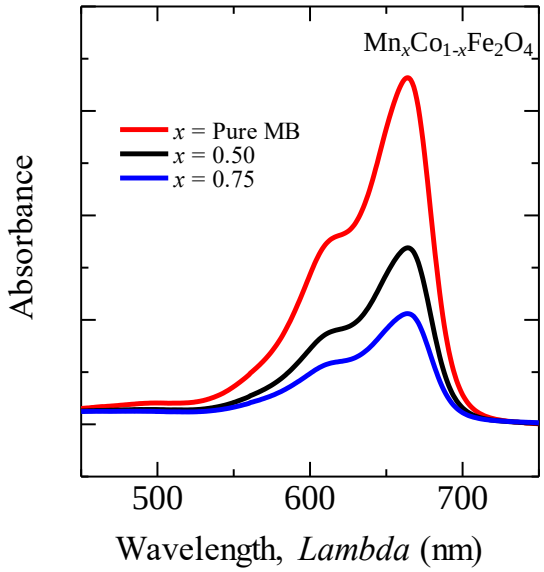

Figure 4. The Absorbtion pattern of the $Mn_xCo_{1-x}Fe_2O_4$ with x = 0.50 and 0.75.

The experiment of photocatalytic activity can be known at the adsorption curves from Figure 4. The Manganese cobalt ferrite indicated that the Methylene Blue (MB) dye solutions of about 49.08% and 68.06% was adsorbed on surface of the samples for x = 0.50 and x = 0.75 after 300 seconds, respectively (Table 4). The adsorption results for the sample x = 0.50 show a low adsorption percentage toward MB dyes removal than sample x = 0.75.

Table 4. Photocatalytic activity of $Mn_xCo_{1-x}Fe_2O_4$ in MB degradation

x	E (%)	k_{app} (1/sec)	$t_{1/2}$ (sec)	E_g (eV)
0.50	49.08	2.25 x 10^{-3}	308.09	180.52 x 10^{-2}
0.75	68.06	3.80 x 10^{-3}	182.22	180.05 x 10^{-2}

Table 4 also show results of calculation from equation 4-6, rate constant (k_{app}) from methylene blue (MB) degradation at the sample with x = 0.75 was higher than the sample wit x = 0.50, i.e. 3.80 x 10^{-3} > 2.25 x 10^{-3} . The half life time ($t_{1/2}$) for photocatalytic reaction in MB dyes solution removal were 308.09 sec and 182.22 sec, where the sample with x = 0.50 was slower than the sample with x = 0.75.

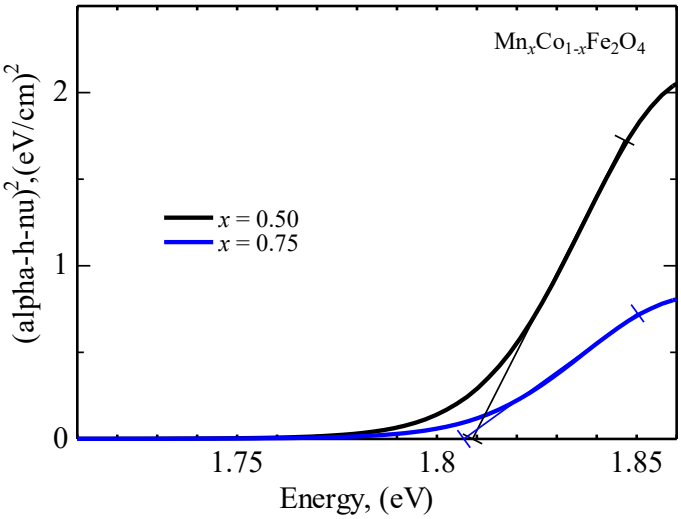

Figure 5. Tauc plot of the $Mn_xCo_{1-x}Fe_2O_4$ with x = 0.50 and 0.75.

From tauc plot that showed by Figure 5, band gap energy of all samples have negative trend. Band gap energy for pure MB solution was 180.97 x 10^{-2} eV, 180.52 x 10^{-2} eV and 180.05 x 10^{-2} eV for MB-MnCo-ferrite solution with x = 0.50 & x = 0.75. The addition of number of Mn content in MB solution reduced band gap energy, respectively. Beside that, the degradation of MB can be caused by magnetic separation of solids from aqueous solution (Dou et al., 2020), which magnetic properties changed with the addition of number of Mn content (Table 3).

The sample x = 0.75 has crystallite size (D) 32.17 nm, this size was smaller than the sample x = 0.50 with 34.85 nm. Thus, the surface area on the sample with small size were larger than the sample with large size, naturally, the sample with large surface area have advantageous for photocatalytic action to involve the adsorption of MB dyes on their surface (Maniammal et al., 2018).

4. Summary

The $Mn_xCo_{1-x}Fe_2O_4$ with x = 0.50 & 0.75 were successfully synthesized by chemical co-precipitation method. The obtained materials confirmed have inverse structures spinel. Addition Mn^{2+} content into samples affects force constant on octahedral site and some crystal structure parameters, i.e. crystallite size and x-ray density decreased, but lattice constant increased. The magnetic properties from the samples also changed. Magnetization saturation and magnetization remanence increased, but the coercive field decreased with rise of presence of Mn^{2+} ions.

Photocatalytic activity show that samples with high Mn content have high adsorption percentage toward MB dyes removal and increase the rate constant of MB degradation. Furthermore,the samples of $Mn_xCo_{1-x}Fe_2O_4$ with x = 0.50 & 0.75 can be applied for photocatalyst of MB degradation.

References

Ahalya, K. N. Suriyanarayanan, V. Ranjithkumar. (2014). Effect of Cobalt Substitution on Structural and Magnetic Properties and Chromium Adsorption of Manganese Ferrite Nano Particles, *J. Magn. Magn. Mater.,* 372 208-213.

Arshad, M. M. Asghar, M. Junaid, M. F. Warsi, M. N. Rasheed, M. Hashim, M. A. Al-Maghrabi, M. A. Khan. (2019). Structural and Magnetic Properties Variation of Manganese Ferrites via Co-Ni Substitution, *J. Magn. Magn. Mater*., 474. 98-103

Ashour, A. H. A. I. El-Batal, M. I. A. A. Maksoud, G. S. El-Sayyad, S. Labib, E. Abdeltwab, M. M. El-Okr. (2018). Antimicrobial Activity of Metal Substituted Cobalt Ferrite Nanoparticles Synthesized by Sol-Gel Technique, *Particuology.*, 40.141-151

Atif, M., M. Idrees, M. Nadeem, M. Shiddique, M. W. Ashraf., (2016). Investigation on The Structural, Dielectric and Impedance Analysis of Manganese Substituted Cobalt Ferrite i.e. Co1-xMnxFe2O4 ($0.0 \leq x \leq 0.4$), *Roy. Soc. Chem*., 620876.

Becyte, V. K. Mazeika, T. Rakickas, V. Pakstas. (2015). Study of Magnetic and Structural Properties of Cobalt-Manganese Ferrite Nanoparticles Obtained by Mechanochemical Synthesis , *Mater. Chem. Phys*. 1-5.

Boda, N. G. Boda, K.C.B. Naidu, M. Srinivas, K. M. Batoo, D. Ravinde, A. P. Reddy. (2019). Effect of Rare Earth Elements on Low Temperature Magnetic Properties of Ni and Co-Ferrite Nanoparticles , *J. Magn. Magn. Mater*., 473.228-235.

Caltun, O. G. S. N. Rao, K. H. Rao, B. P. Rao, I. Dumitru, C. O. Kim, C. Kim, (2007). The Influence of Mn Doping Level on Magnetostriction Coefficient of Cobalt Ferrite, *J. Magn. Magn. Mater*., 316.e618-e620

Cojocariu, A. M. M. Soroceanu, L. Hrib, V. Nica, O. F. Caltun. (2012). Microstructure and Magnetic Properties of Substituted (Cr, Mn) – Cobalt Ferrite Nanoparticles, *Mater. Chem. Phys.,* 135 728-732

Doaga, A. A. M. Cojocariu, W. Amin, F. Heib, P. Bender, R. Hempelmann, O. F. Caltun. (2013). Synthesis and Characterizatons of Manganese Ferrites for Hyperthermia

Applications, *Mater. Chem. Phys*., 143.305-310.

Dou, R. H Cheng, J Ma, S Komarneni. (2020). Manganese doped magnetic cobalt ferrite nanoparticles for dye degradation via a novel heterogeneous chemical catalysis, *Mater. Chem. And Phys*. 240 122181.

Enrico. C. (2017). Advanced Magnetic and optical materials, in: Asuthosh Tiwari et al (Eds.), *Magnetic Nanomaterial-Based Anticancer Therapy*, Scrivener Publishing LLC, Beverly. pp. 141-164

Flores, V. C. D. B. Baques, A. V. Glushchenko, R. F. Ziolo, J. A. M. Aquino, R. S. Turtelli, R. Grossinger. (2015). Magnetic Properties of Spinel Cobalt-Manganese Ferrites, *IEEE Trans. Magn.,* Vol. 51, No. 4,

Forgacs, E. T Cserhati, G Oros. (2004). Removal of synthetic dyes from wastewaters: a review, *Env. Int*. 30.953–971.

Ghahfarokhi, S E. E M Shobegar. (2018). Structural, magnetic, dielectric and optical properties of $Sr_{1-x}Mn_xFe_2O_4$ nanoparticles fabricated by sol-gel method, *J. of Alloy. And Comp.* 76865-73

Gul, M. & K. Akhtar. (2018). Synthesis and Characterization of Al-doped Manganese Ferrite Uniform Pasrticles for High-Frequency Applications, *J. Alloys and Comp.*765.1139-1147

Hou, X. J. Feng, X. Xu, M. Zhang. (2010). Synthesis and Characterization of Spinel MnFe2O4 Nanorod by Seed-Hydrothermal Route, *J. Alloys and Comp*., 491 258-263.

Jabbar, R. S. H. Sabeeh, A. M. Hameed. (2019). Stuctural, Dielectric and Magnetic Properties of Mn^{2+} Doped Cobalt Ferrite Nanoparticles, *J. Magn. Magn. Mater*., 31215-6

Karaagac, O. B. B. Yildiz, H. Kockar. (2019). The Influence of Synthesis Parameters on One-Step Synthesized Superparamagnetic Cobalt Ferrite Nanoparticles with High Saturation Magnetization, *J. Magn. Magn. Mater*., 473. 262-267.

Koseoglu, Y. F. Alan, M. Tan, R. Yilgin, M. Ozturk. (2012). Low Temperature Hydrothermal Synthesis and Characterization of Mn Doped Cobalt Ferrite Nanoparticles, *Ceram. Int*., 38. 3625-3634

Kotnala, R. K. & J. Shah. Ferrite Material: Nano to Spintronics Regime, in: *Handbook of Magnetic Materials*, Vol. 23, 2015.

Liu, B. H. J. Ding, Z. L. Dong, C. B. Boothroyd, J. H. Yin, J. B. Yi. (2006). Microstructural Evolution and Its Influence on The Magnetic Properties of $CoFe_2O_4$ Powders During Mechanical Milling Microstructural Evolution and Its Influence on The Magnetic Properties of $CoFe_2O_4$ Powders During Mechanical Milling, *Phys. Rev*. B, 74.184427.

Lungu, A. I. Malaescu, C. N. Marin, P. Vlazan, P. Sfirloaga. (2015). The Electrical Properties of Manganese Ferrite Powders Prepared by Two Different Methods, *Physica B.,* 462. 80-85.

Magone, E. M K Kim, H J lee, J H Park. (2018). Testing and Substantial Improvement of TiO2/UV Photocatalysts in The Degradation of Methylene Blue, *Ceram. Int.*

Maniammal, K. G Madhu, V Biju. (2018). Nanostructured mesoporous NiO as an

efficient photocatalyst for degradation of methylene blue: Structure, properties and performance, *Nano-Struc. & Nano*-Ob. 16 266-275

Marcu, A. S. Pop, F. Dumitrache, M. Mocanu, C. M. Niculite, M. Ghergicheanu, C. P. Lungu, C. Fleaca, R. Ianchis, A. Barbut, C. Grogoriu, I. Morjan. (2013). Magnetic Iron Oxide Nanoparticles as Drug Delivery System in Breast Cancer, *J. Appl. Surf. Sci.*

Masunga, N. O K Mmelesi, K K Kefeni, B B Mamba. (2019). Recent Advance in Copper Ferrite Nanoparticles and Nanocomposites Synthesis, Magnetic Properties and Application in Water Treatment : *Review, J. of Env. Chem. Eng*., 7. 103179

Montgomery, M A. M Elimelech. (2007). Water and sanitation in developing countries: including health in the equation, *Env. Sci. Tech.*

Mostafa, N. Y. Z. I. Zaki, Z. K. Heiba. (2013). Structutal and Magnetic Properties of Cadmium Substituted Manganese Ferrites Prepared by Hydrothermal Route, J. Magn. *Magn. Mater*., 329.71-76.

Mota, A L N. L F Albuquerque, L T C Beltrame, O Chiavone-Filho, A Machulek Jr., C A O Nascimento. (2009). Advanced oxidation processes and their application in the petroleum industry: a review, *J. Pet. Gas*.

Nasrin, S. F. U. Z. Chodhury, S. M. Hoque. (2019). Study of Hyperthermia Temperature of Manganese-Subtituted Cobalt Nano Ferrites Prepared by Chemical Co-Precipitation Method for Biomedical Application, *J. Magn. Magn. Mater*., 479 126-134.

Pakzad, K. H Alinezhad, M Nasrollahzadeh. (2019). Green synthesis of Ni@Fe3O4 and CuO nanoparticles using Euphorbia maculata extract as photocatalysts for the degradation of organic pollutants under UV-irradiation, *Ceram. Int.* 45 17173-17182.

Purnama, B. A. T. Wijayanta, Suharyana. (2018). Effect of Calcination Temperature on Structural and Magnetic Properties in Cobalt Ferrite Nano Particles, *J. King Saud Univ*.

Samavati, A. A F Ismail. (2017). Antibacterial properties of Copper-substituted cobalt ferrite nanoparticles synthesized by co-precipitation method, *Particuology* 30 158-163

Saputro, D E. Utari, B Purnama. (2019). XRD and FTIR analysis of bismuth substituted cobalt ferrite synthesized by co-precipitation method, *IOP Conf. Ser.: J. of Phy:Conf. Ser. 1153*.012057

Sonu, V Dutta, S Sharma, P Raizada, A H Bandegharaei, V K Gupta, P Singh. (2019). Review on augmentation in photocatalytic activity of $CoFe_2O_4$ via heterojunction formation for photocatalysis of organic pollutants in water, *J. of Saudi Chem. Soc*.

Swatsitang, E., S. Phokha, S. Hunpratub, B. Usher, A. Bootchanont, S. Maensiri, P. Chindaprasirt. (2016). *J. Alloys. Comp*., 664.792-797.

Tsay. C. Y. Y. H. Lin, S. U. Jen. (2014). Magnetic, Magnetostrictive, and AC Impedance Properties of Manganese Substituted Cobalt Ferrites, *Ceram. Int*., 020501-1.

Vlazan, P. I. Miron, P. Sfirloaga. (2014). Cobalt Ferrite Subituted with Mn: Synthesis

Method, Characterization and Magnetic Properties, *Ceram. Int*.

Xi G. & Y. Xi. (2016). Effects on Magnetic Properties of Different Metal Ions Substitution Cobalt Ferrites Synthesis by Sol-gel Auto-combustion Route Using Used Batteries, *Mater. Lett*., 164.444-448.